

Calculation of Sievert Integral for Point-Kernel Shielding Applications

Mario Matijević, Andrea Kaselj, Krešimir Trontl
University of Zagreb, Faculty of Electrical Engineering and Computing
Unska 3, 10000 Zagreb, Croatia
mario.matijevic@fer.hr, andrea.kaselj@fer.hr, kresimir.trontl@fer.hr

ABSTRACT

The application of a point-kernel technique in gamma radiation shielding calculations has a long and successful history. Using this approach radiation sources of various shapes such as point, linear, planar, or volumetric can be subdivided using the linear superposition principle to calculate total radiation received at a detector. Mathematically, any form of a distributed source may be treated as a summation i.e. integration of the radiation received from an equivalent number of point sources, for which exponential point-kernel function is analytically known. Fundamental assumption is that there is no interaction of individual point sources which together represent total distributed radiation source. The effects of geometrical boundaries and gamma scattering are not included in this treatment, so users should be aware of these inherent limitations when comparing with reference results, such as Monte Carlo (MC) solution. This paper presents a specific case of gamma flux attenuation from a distributed line source of photons in front of a slab shield, but is actually part of a larger effort, whose final goal is a general-purpose point-kernel code development. The solution of a line source with a slab shield is known as the secant or Sievert integral, which cannot be evaluated analytically, so auxiliary tabulated function is introduced to facilitate bilinear interpolation on angle and shield thickness. Such a code, written in C-language, will provide graphical user interface to assist user with necessary input data preparation and selection of predefined shielding materials for which Taylor buildup factors are provided. This paper gives programming and numerical aspects of such point-kernel code for which results of the test cases are compared with an MC solution of SCALE6.1.3 code package.

Keywords: *point-kernel, line source, gamma radiation, shielding, buildup factors*

1 INTRODUCTION

The point-kernel method in radiation shielding originates from the early days of reactor projects which clearly demonstrated how shield design for neutrons and gamma rays place significant problems regarding price, size and efficient flux attenuation. Starting with first organized research program in reactor shielding (end of 1940-ties in USA) it was soon recognized that the radiation streaming through ducts and holes together with secondary gamma heating effects in the shield will greatly influence the overall shielding design. The Oak Ridge National Laboratory (ORNL) conducted pioneering research investigation that led to the concept of the fast neutron removal cross section, which quickly came into widespread use for neutron attenuation problems. After that, the pool-type research reactors were constructed and provided numerous basic and applied results of shielding materials. The cancelation of the USA aircraft nuclear propulsion program and successful nuclear submarine program (1950-ies) gave a rich development of shield-analysis methods (point-kernel, method of moments, removal-diffusion, gamma-ray buildup factors, etc.) together with new experimental facilities being built worldwide. Simultaneously, early papers

of H. Kahn [1] from Rand Corporation on the Monte Carlo (MC) application for radiation shielding showed a new, alternative approach, but scarcity of the first digital computers deferred widespread use of this new stochastic technique, which was also investigated in ORNL and LASL (Los Alamos Scientific Laboratory). The numerical techniques for solving Boltzmann transport equation were concurrently investigated and the most notable one was B. Carlson's method of LASL known as discrete ordinates SN originating from mid 1950-ies [2]. After that, improvements in SN method on spatial differencing and various convergence techniques followed, giving a well known ANISN code of ORNL in 1965 which was also suitable for shielding calculations. In mid 1960-ies there were already eight major MC programs in use only in USA, which confirmed many analytical solutions for shielding configurations originating from an older point-kernel approach, which was still a standard shielding method of those days.

The important historical event from that period was also foundation of Radiation Shielding Information Computational Center (RSICC) in ORNL 1962, which still serves its original mission to promote development of new nuclear codes and data for shielding community. A more detailed historical exposition can be found in [3], but it suffice to say how even today point-kernel methods have their place in many preliminary shielding studies, before reaching to accurate MC or SN methods, giving a fast solution of the problem but within a well known theoretical constraints.

The rest of the paper is organized as follows. Chapter 2 gives formal point-kernel definition for gamma ray shielding with presentation of exponential point kernel and buildup factors. Chapter 3 presents the problem of radiation attenuation from a line source which leads to a Sievert integral solution. The programming details of the point-kernel program for a line gamma source and a slab shield are presented in Chapter 4, together with graphical user interface (GUI) development to assist users with input data. The comparison of gamma ray shielding results from the point-kernel and Monaco MC code of SCALE6.1.3 is presented in Chapter 5, while conclusions are given in Chapter 6. A list of references is given at the end of the paper.

2 THE POINT-KERNEL METHOD

The point-kernel method or mathematically speaking method of Green's function, is one of the oldest and widely used methods for the solution of both neutron and gamma-ray shielding problems [3][4][5]. Using this approach radiation sources of various shapes such as point, linear, planar, or volumetric can be subdivided using the linear superposition principle to calculate the total radiation received at a detector. Mathematically, any form of a distributed source may be treated as a summation i.e. integration of the radiation received from an equivalent number of point sources, for which exponential point-kernel function is analytically known. Fundamental assumption is that there is no interaction of individual, point sources which together represent total distributed radiation source. The effects of geometrical boundaries and gamma scattering are not included in this treatment, so users should be aware of these inherent limitations when comparing with reference results, such as Monte Carlo (MC) solution.

The point-kernel principle is the following [6]: the radiation received at the detector (or other receptor) from a distributed source may be treated as a summation (or integration) of the radiation received from an equivalent number of point sources. The point-kernel function $G(|\vec{r}' - \vec{r}|)$ is defined as the response of a detector at the space point r coming from a point source of radiation located at r' emitting one particle per second. The source strength $S(\vec{r}')$ can be for a line, surface or volume configuration and if we consider small source element $d\vec{r}'$ (increment of length, area or volume) then we can construct a point source emitting particles at the rate of $S(\vec{r}')d\vec{r}'$. The differential response of a point detector located at \vec{r} is simply:

$$d\phi(\vec{r}) = G(|\vec{r}' - \vec{r}|)S(\vec{r}')d\vec{r}'. \quad (1)$$

The total response of an isotropic point detector is obtained by integrating Eq. (1) over the whole finite source space as the

$$\phi(\vec{r}) = \int_{source} G(|\vec{r}' - \vec{r}|) S(\vec{r}') d\vec{r}'. \quad (2)$$

One should notice how the point-kernel function depends on a source-detector distance, on particle type, its energy, and materials covering intervening path of radiation. If a G -function can be obtained in a fairly simple form, such as exponential form, one could perform integration for distributed sources leading to useful results in radiation attenuation. This is typically done by considering a point isotropic emitter of S_p monoenergetic particles per second, for which uncollided particle flux is given as the inverse square law over a hypothetical surface sphere of radius R :

$$\phi(R) = \frac{S_p}{4\pi R^2} \exp(-\mu R). \quad (3)$$

The exponential attenuation of a shielding material between the source and the detector is described with a linear attenuation coefficient μ (cm^{-1}), R is the line distance while μR is the number of gamma ray mean free paths. Taking the definition of point-kernel from Eq. (3) one can notice that the exponential kernel for the uncollided flux from a point source is given by

$$G(R) = \frac{\exp(-\mu R)}{4\pi R^2}. \quad (4)$$

This result is correct for a relatively thin layer of attenuating material, especially for photons of high energy, meaning there is a small probability of scattered photons reaching the detector. For practical purposes, gamma shields are always "thick", so after a multiple scattering there is a certain probability of photon reaching the detector, giving a higher measured flux that exceeds the uncollided flux. Allowance of scattered flux reaching the detector is done by multiplicative buildup factor $B > 1$, which is a function of the number of mean free paths and photon energy. The total measured (buildup) flux will then consist of collided and uncollided part, so for point source of monoenergetic gamma rays S_p and distance R in shielding medium flux is given as

$$\phi(R) = \frac{S_p}{4\pi R^2} \exp(-\mu R) B(\mu R, E_\gamma), \quad (5)$$

while the corresponding point-kernel is

$$G(R) = \frac{\exp(-\mu R) B(\mu R, E_\gamma)}{4\pi R^2}. \quad (6)$$

The concept of buildup factors can be, at least in general, applied to both gamma rays and neutrons [7][8], but for practical purposes it is mainly used for gamma-ray attenuation calculation due to complex neutron interactions. Advancing the machine learning algorithms, there is also an incentive to integrate such artificial intelligence algorithms inside the point-kernel paradigm [9]. In the case of fast neutrons, it introduces fast neutron removal cross sections. Tables of buildup factors are readily available as a function of gamma ray energy and shield thickness (in mean free paths) and should be differentiated for point source and planar source. When performing integration of distributed sources, it is often necessary to express buildup factors in analytical form, so in this paper we are using a well-known Taylor form given as:

$$B(\mu R, E_\gamma) = A \exp(-\alpha_1 \cdot \mu R) + (1 - A) \exp(-\alpha_2 \cdot \mu R), \quad (7)$$

where A , α_1 , and α_2 denote coefficients readily found in tabulated form for different shielding material and incident gamma ray energy. This function will later be combined with the point exponential kernel when deriving expressions for a gamma flux from a line source and a slab shield. Parameters of the Taylor form can be found in the classical radiation shielding references [3][5].

3 RADIATION ATTENUATION FROM A LINE SOURCE

This section presents application of point-kernel method to a gamma line source [6] emitting S_1 particles/cm/s. If we take a differential element of line length dl (cm) then the product $S_1 \cdot dl$ represents point gamma source (particles/s). The detector response at distance R is then given by point-kernel definition as integration over the length l of the source:

$$\phi(R) = \int_l S_1 G(R) dl. \quad (8)$$

This result is completely general, so an actual problem setup is needed to perform specific integration. One should bear in mind how effects of problem boundaries are not included, and gamma rays, which may be scattered multiple times in shield before reaching the detector, are modeled by means of buildup factors. We are considering a long line representing linear isotropic radiator of photons in front of a slab shield with thickness t (see Figure 1).

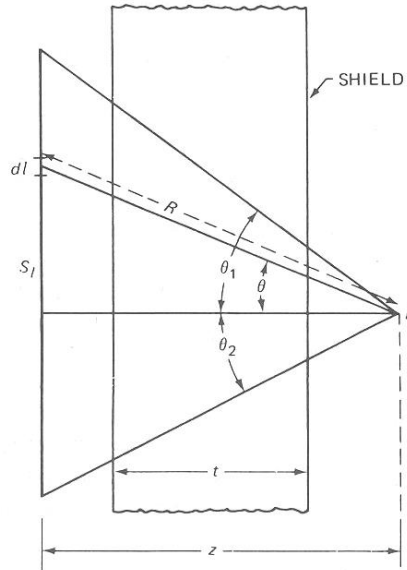


Figure 1: Point detector response from gamma line source [6]

The exponential point kernel of Eq. (4) is substituted in Eq. (8) for a general line source. The distance R for any point source to the detector is expressed in perpendicular distance from the line source to the detector P (variable z) and angle θ , i.e. $R = z \cdot \sec \theta$. The point-kernel function for the uncollided flux (B factor equal to 1) is written as a function of variables z , t , and θ , giving

$$G(z, t, \theta) = \frac{\exp(-\mu t \cdot \sec \theta)}{4\pi R^2} = \frac{\exp(-\mu t \cdot \sec \theta)}{4\pi (z \cdot \sec \theta)^2}. \quad (9)$$

To perform point-kernel integration, we express differential line element dl as a function of variables z and θ . This is done first by derivation of expression $R^2 = z^2 + l^2$, giving $l \cdot dl = R \cdot dR$.

The same is repeated for differential element dR , i.e. the derivation of $z = R \cos \theta$ is giving $dR = (l \cdot d\theta) / \cos \theta$. Combining obtained expressions, we eliminate l variable and finally get

$$dl = z \cdot (\sec \theta)^2 d\theta. \quad (10)$$

This permits two-part integration over the whole line length in terms of angle θ , i.e. from 0 to θ_1 and from 0 to θ_2 :

$$\phi(R) = \int_l S_l G(R) dl = \int_l S_l \frac{\exp(-\mu t \cdot \sec \theta)}{4\pi(z \cdot \sec \theta)^2} z \cdot (\sec \theta)^2 d\theta. \quad (11)$$

$$\phi(R) = \frac{S_l}{4\pi z} \int_l \exp(-\mu t \cdot \sec \theta) d\theta = \frac{S_l}{4\pi z} \left[\int_0^{\theta_1} e^{-\mu t \cdot \sec \theta} d\theta + \int_0^{\theta_2} e^{-\mu t \cdot \sec \theta} d\theta \right]. \quad (12)$$

It is customary to introduce the secant or Sievert integral defined as $F(\theta, x) = \int_0^\theta e^{-x \cdot \sec \theta} d\theta$, so uncollided flux solution can be finally expressed as:

$$\phi_l(z, t) = \frac{S_l}{4\pi z} [F(\theta_1, \mu t) + F(\theta_2, \mu t)]. \quad (13)$$

Plots of Sievert integral are usually find in standard radiation shielding handbooks [3][4] for various values of (θ, x) or in tabulated values of auxiliary function $\bar{F}(\theta, x)$ as $F(\theta, x) = \theta e^{-x} \bar{F}(\theta, x)$ or in form of several series expansion with different and limited values of (θ, x) . For purposes of programming, the tabulated F -function approach was selected.

To obtain the total flux solution, one must include the buildup factor $B(\mu t \cdot \sec \theta)$ in exponential point-kernel and again perform integration. For that purpose, we are using Taylor form of buildup factors as:

$$B = A \exp(-\alpha_1 \mu t \cdot \sec \theta) + (1 - A) \exp(-\alpha_2 \mu t \cdot \sec \theta). \quad (14)$$

The corresponding point-kernel for buildup flux is thus

$$G(z, t, \theta) = \frac{1}{4\pi(z \cdot \sec \theta)^2} [A e^{-\mu t \cdot \sec \theta (1 + \alpha_1)} + (1 - A) e^{-\mu t \cdot \sec \theta (1 + \alpha_2)}], \quad (15)$$

while the total or buildup flux from gamma line source becomes

$$\phi_l(z, t) = \frac{S_l}{4\pi z} \left[A \{F(\theta_1, \mu t(1 + \alpha_1)) + F(\theta_2, \mu t(1 + \alpha_1))\} + (1 - A) \{F(\theta_1, \mu t(1 + \alpha_2)) + F(\theta_2, \mu t(1 + \alpha_2))\} \right]. \quad (16)$$

For practical purposes, this buildup flux of photons originating from a gamma line source and penetrating a slab shield configuration can be expressed as a relative ratio to the uncollided flux component, giving the so called numerical approximation of the buildup factor, which can be easily compared to other (theoretical) buildup factors set, such as Taylor or Goldstein [3][5]:

$$B = \frac{\phi_{tot}}{\phi_{unc}} = \frac{(1-A)\{F(\theta_1, \mu t(1+\alpha_2)) + F(\theta_2, \mu t(1+\alpha_2))\}}{F(\theta_1, \mu t) + F(\theta_2, \mu t)} \quad (17)$$

The presented equations for a gamma line source and a slab shield are used for programming the point-kernel code which can be used in two different ways: a) shield thickness is a known input parameter, buildup flux is searched on point detector; b) buildup flux on point detector is a known input parameter, shield thickness is searched. In the later case, which is a more difficult one, iterative algorithm with predefined precision is used for a numerical solution.

4 THE POINT-KERNEL CODE DEVELOPMENT

The C-programming language [10] was used as a standard tool for coding numerical routines which solve gamma line equations presented in the previous Chapter. The exposure buildup factors for point gamma source (i.e. Goldstein data set) as well as coefficients of Taylor form were used from classic references [3][5], together with mass attenuation data and densities of several shield materials [6]: water, concrete, aluminum, iron, tin, lead and depleted uranium. The linear interpolation C function was written for calculation of mass attenuation coefficients and for Taylor coefficients, since the user provides floating point value for gamma ray energy in MeV. The bilinear interpolation routine was written for calculation of F-function values and Goldstein buildup factors. These user-defined C functions are floating point type with several arguments of floating-point values and pointers on data sets. For example, the function prototype of bilinear interpolation on Goldstein set is given as the float type function with float pointers on buildup factors matrix, energy vector, shield thickness vector, user-defined energy, and user-defined shield thickness:

```
float BilinInt(float *tablica, float *ene, float *deb, float Eg, float mfp);
```

The users are prompted to select and enter several input variables describing the basic shielding problem: shielding material (1 to 7), gamma ray energy in range [0.5 - 10] MeV, gamma line specific intensity (phot/cm/s), perpendicular distance from gamma line to a point detector, and a gamma line length (upper and lower part, in cm). The selection of shielding materials (on left) and gamma line parameters (on right) is shown in Figure 2.



Figure 2: Example of user entry values

The user input data are accompanied with partial on-screen printout of intermediate results, such as mass attenuation coefficient, gamma ray mean free path (mfp) in shield, Taylor form coefficients, F-function or Sievert integral values, Goldstein buildup factors, etc. The example of such intermediate results is shown in Figure 3 for an asymmetric gamma line with a total length of 125 cm and bilinear interpolation of 10.78 for Goldstein buildup factor.

```

.....
Table F(theta,x) Shure and wallace 1975.
x(#mfp): [0.01 - 75.0]
theta(deg): [1.0 - 90.0]
.....

Upper line length l1(cm) > 0: 50
>>> theta1 = 26.57 st
>>> F(26.57,6.52) = 5.49e-004

Lower line length l2(cm) > 0: 75
>>> theta2 = 36.87 st
>>> F(36.87,6.52) = 6.36e-004

>>> Goldstein B-factor:
Energy 0.50 Mev is from interval [0.50, 1.00] Mev.
Shield thickness (mfp) 6.516360 is from interval [4.00, 7.00].
Bilinear interpolation: 10.777860

```

Figure 3: Example of intermediate results

The compiled point-kernel program can be run in two basic modes:

a) *Direct solution variant* (or "easy solution") - users enter slab shield thickness (in cm) while the program calculates three types of buildup factors (Goldstein, Taylor and numerical) and buildup gamma flux on point detector, based on user input data.

b) *Iterative solution variant* (or "hard solution") - users enter buildup flux on a point detector (phot/cm²/s) while the program calculates three types of buildup factors (Goldstein, Taylor and numeric) and slab shield thickness, based on user input data.

In both cases the program will print out information on the relative flux ratio, i.e. uncollided flux divided over buildup flux, providing information about the importance of photon scattering inside the shield. The program finally prints information about CPU timing in ms and sec, based on different built-in C functions defined in "sys/timeb.h" and "time.h" libraries. Figure 4 shows results of the direct solution variant using the following input parameters: iron shield 10 cm thick, gamma ray energy 0.5 MeV, specific gamma source of 1e6 phot/cm/s, total line length of 125 cm (50 cm above z=0 cm plane and 75 cm below), and line-to-detector distance of 100 cm. One can notice how the flux ratio of uncollided to total is about 9.33% so by inverting this value one can simply obtain so-called numerical buildup factor, which is similar to a well-known theoretical value of Goldstein and Taylor.

```

*****
*** POINT-KERNEL RESULTS ***
*** (direct solution variant) ***
*****
Gamma line spec.intensity: 1.000e+006 phot/cm/s.
Gamma line energy: 0.500000 Mev.
Shield density: 7.870000 g/cm3.
Mass atten.coefficient: 0.082800 cm2/g.
Linear atten.coefficient: 0.651636 1/cm.
Gamma ray mfp in shield: 1.534599 cm.
Shield thickness in #mfp: 6.516360.
Shield thickness in cm: 10.000000.

Goldstein buildup factor: 10.777860.
Taylor buildup factor: 10.240284.
Numerical buildup factor: 10.719247.

Buildup flux: 1.01e+001 phot/cm2/s.
Uncollided flux: 9.43e-001 phot/cm2/s.
Flux ratio unc/tot = 9.329014 %.
*****

```

Figure 4: Main output values - direct solution

If the same setup problem is re-run in iterative solution variant, where users enter a known buildup flux of 10.1 phot/cm²/s, then the shield thickness of 10.002086 cm is obtained through 5518 iterations with total CPU time of 15 ms for the initial shield thickness of 1 mfp (allowed range is 0.01 - 75 mfp). In the worst-case scenario, if the users enter initial value for the shield thickness of 75 mfp, the number of iterations increases to 68512 with total CPU of 110 ms, which is a factor of 7

increase. The iterative solution results for the same problem are shown in Figure 5. The users can easily change numerical ϵ -values which control desired solution precision and have direct influence on iteration number and CPU timing.

```

*****
*** POINT-KERNEL RESULTS ***
*** (iterative solution variant) ***
*****
Gamma line spec.intensity: 1.000e+006 phot/cm/s.
Gamma line energy: 0.500000 MeV.
Shield density: 7.870000 g/cm3.
Mass atten.coefficient: 0.082800 cm2/g.
Liner atten.coefficient: 0.651636 1/cm.
Gamma ray mfp in shield: 1.534599 cm.
Shield thickness in #mfp: 6.517301.
Shield thickness in cm: 10.001444.

Goldstein buildup factor: 10.779654.
Taylor buildup factor: 10.242074.
Numerical buildup factor: 10.721163.

Iterations counter: 68512.
Buildup flux: 1.01e+001 phot/cm2/s.
Uncollided flux: 9.42e-001 phot/cm2/s.
Flux ratio unc/tot = 9.327346 %.

*****
***** CPU wall time in sec / ms *****
*****
---<function clock() from time.h>---
wall time for 68512 iterations: 1.09e-001 sec.
wall time per iteration: 1.59e-006 s.
---<function ftime() from timeb.h>---
wall time for 68512 iterations: 1.10e+002 ms.
wall time per iteration: 1.61e-003 ms.
*****

```

Figure 5: Main output values - iterative solution

The final effort was put into a graphical user interface (GUI) development, written in C++ language [11] as a desktop application using Qt cross-platform [12] development framework as widget toolkit. The GUI is an interface program between precompiled executable modules and text-based input and output files. The main window in Figure 6 is a tab Widget which holds all open tabs. For both calculation variants there are input data fields, option to save the result to a text file, scheme of geometric configuration, result field, status and output fields and options to generate graphs by running the C application in a loop. The program displays and exports graphs for selected ranges of input data and provides a display of previously saved calculations in a separate tab. All input data are checked when pressing "Calculate" button and any error messages are shown in the status field. This software was implemented with the aim to enable further development by adding new components such as other source geometric configurations and visualization elements.

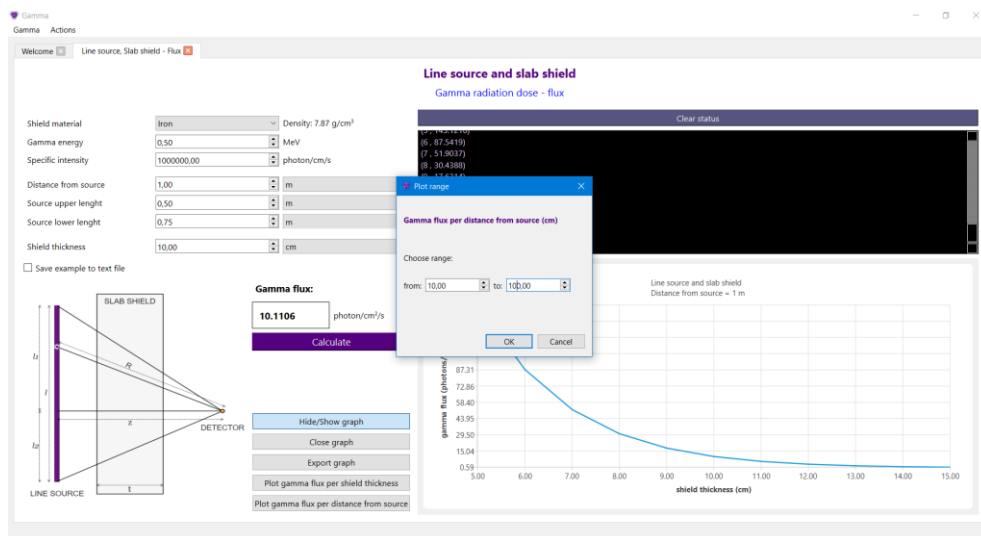


Figure 6: The main window of the GUI program

5 COMPARISON OF POINT-KERNEL AND MC SOLUTION

The point-kernel solution of isotropic gamma line with an iron slab shield was compared with a reference MC solution of the same model using the MAVRIC shielding sequence of the SCALE6.1.3 code package [13]. The proposed benchmark was defined as in the previous chapter: isotropic gamma line source emitting photons of energy 0.5 MeV, with specific source intensity of $1e6$ phot/cm/s, total line length of 125 cm (50 cm above $z=0$ cm plane and 75 cm below), and line-to-detector distance of 100 cm. The center of the slab shield was always positioned symmetrically between the line and the point detector. The series of calculations were done for the varying slab shield thickness in cm (1, 5, 10, 20, 30, 40, and 50) and for two gamma line energies in MeV (0.5 and 10), enveloping all other values of available buildup factors. The Monaco MC module was used with the following parameters: "v7-27n19g" cross section library, total gamma source of $1.25e8$ phot/sec, point detector tally estimator 100 cm from the gamma line, 300 batches with 10000 photons per batch. The CADIS variance reduction (VR) methodology was used only for those cases of a relatively thick shield with 0.5 MeV photons, while for other cases MC was run in an analog mode. The average MC relative error on point detector for all simulation cases was well below 0.1 % and CPU time took 6-9 minutes per MC simulation. The selected results of 0.5 MeV gamma rays are presented next. Figure 7 shows gamma buildup flux calculated by point-kernel and MC method with varying shield thickness, with noticeable flux difference starting above 30 cm thickness, which is a satisfactory overall behavior.

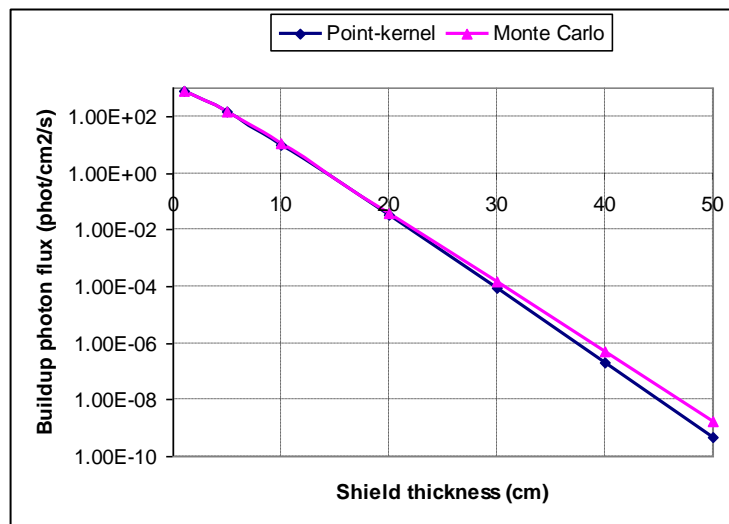


Figure 7: Gamma buildup flux with point-kernel and MC (0.5 MeV photons)

The ratio of uncollided to buildup gamma flux is shown in Figure 8 separately for point-kernel and MC solution, both exhibiting a similar profile, i.e. for shields thicker than 10 cm one can notice how uncollided flux component is below 10% in total flux, so photon scattering becomes a dominant process inside the shield. One can thus expect high-value buildup factors in this scenario.

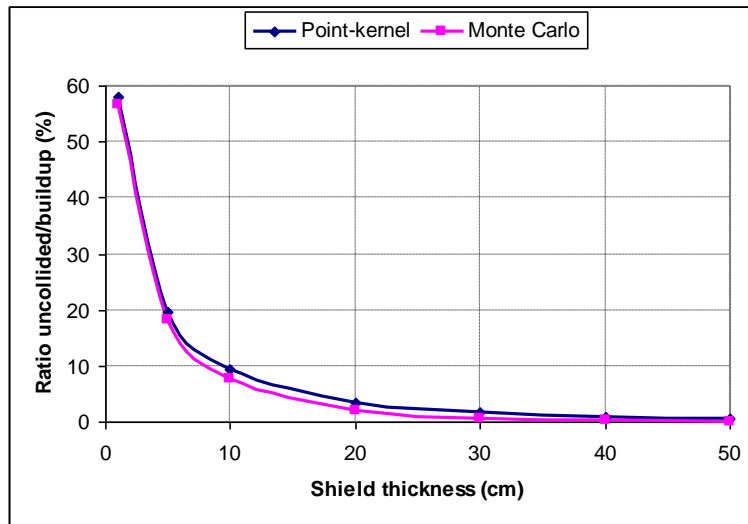


Figure 8: Ratio of uncollided to total gamma flux (0.5 MeV photons)

Figure 9 shows relative error of point-kernel flux to an average MC flux; comparison is done separately for uncollided and buildup gamma flux. One can notice different trends of this curves with increasing shield thickness, i.e. more conservatism comes from the uncollided point-kernel flux and from the total MC flux. These noticeable differences have an origin in the MC particle transport, capturing many physical interactions of 0.5 MeV photons which are neglected in a simple point-kernel integration technique. For practical shielding purposes, one should be concerned only with iron shields up to cca. 20 cm (for example RPV), where point-kernel method exhibits relative error up to 20% , which is an acceptable deviation from the MC solution.

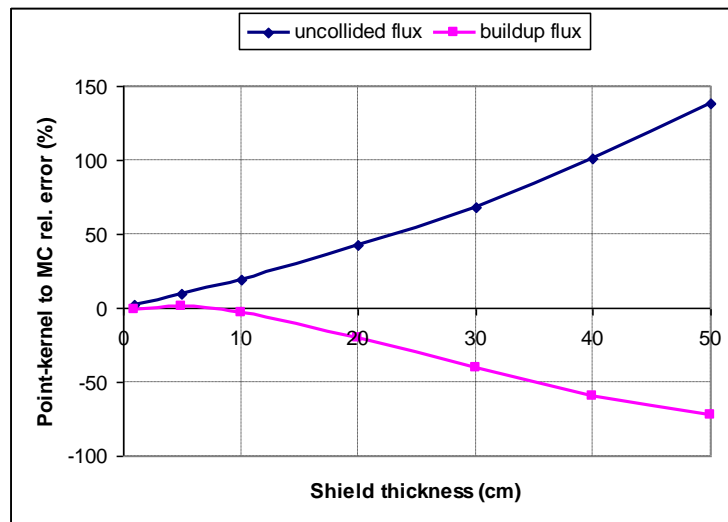


Figure 9: Relative error of point-kernel to MC solution (0.5 MeV photons)

Finally, the buildup factors of 0.5 MeV photons are shown in Figure 10 as a shield thickness function and exhibit a well-known exponential increase. A good agreement between numerical and theory-based buildup factors has been obtained, with no systematic deviations in curve trends.

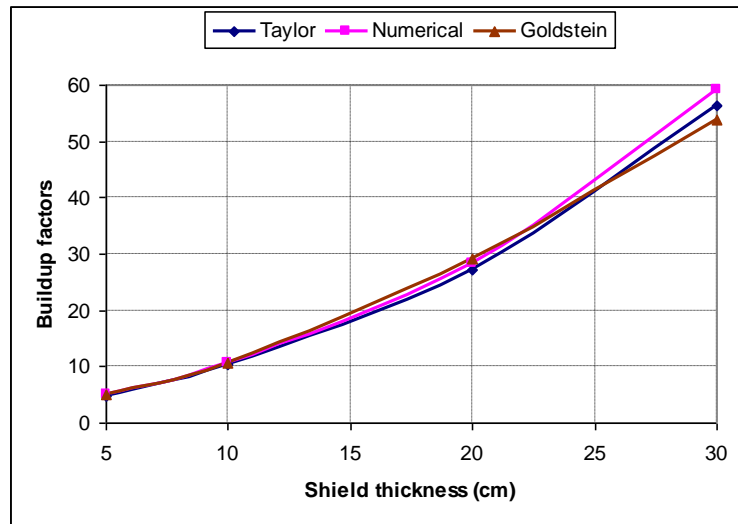


Figure 10: The buildup factors for 0.5 MeV photons inside iron shield

For completeness, the mesh tally of MC gamma buildup flux with relative errors is shown in Figure 11 in $y=0$ plane, corresponding to case of 50 cm iron shield and 0.5 MeV photons. This is an example of deep-penetration gamma ray shielding problem, where effective VR techniques must be used, due to MC statistical constraints on point detector tally estimator. For this case, additional CPU time of 12.5 minutes is needed for the CADIS deterministic solution and VR preparation, so total CPU time amounts to 21 minutes. The MC buildup flux on point-detector is $1.77e-09$ phot/cm²/s with rel. error of 0.93%. For comparison, the point-kernel solution gives a smaller flux value of $0.48e-09$ phot/cm²/s with CPU time of cca 20 ms, since only a one-pass through program is needed to obtain an analytical solution. This is about 63000 times faster than MC solution, with an acceptable flux disagreement, since the solution is order of $\sim 1e-09$.

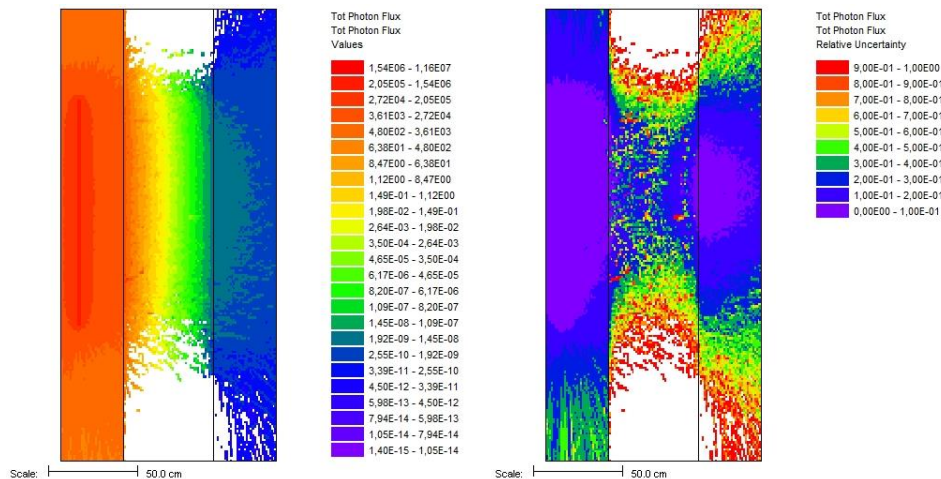


Figure 11: CADIS solution for 0.5 MeV photons and 50 cm thick iron shield

The selected results of 10 MeV gamma ray penetration exhibit different physical behavior since pair-production and photonuclear reactions become a more probable processes for high-energy photons inside the iron shield. Figure 12 shows buildup gamma flux calculated by point-kernel and MC method with varying shield thickness. The curve trends are similar with a constant offset (factor of few) of point-kernel flux values below MC values.

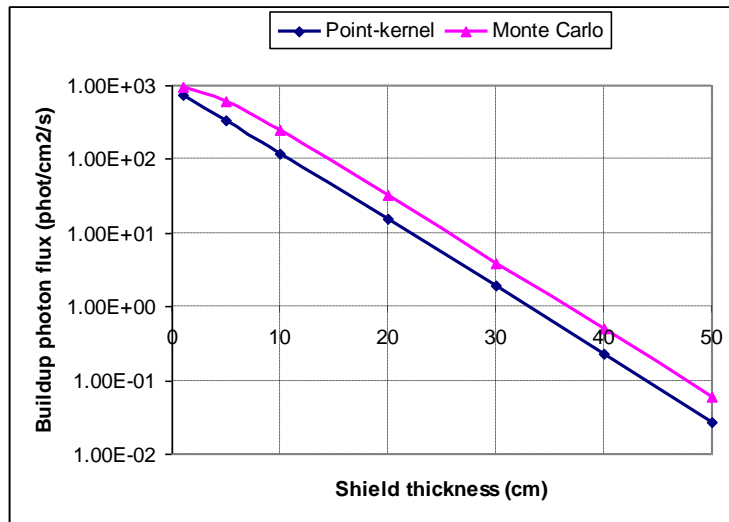


Figure 12: Gamma buildup flux obtained with point-kernel and MC (10 MeV photons)

The ratio of uncollided to total flux is shown in Figure 13, separately for a more conservative point-kernel and MC solution. Since energetic 10 MeV photons will penetrate iron shield more easily than 0.5 MeV photons, one can notice how gamma ray scattering becomes less pronounced. For example, in the case of 10 cm iron shield, this ratio is now over 60% for point-kernel solution and 30% for MC solution. In the case of 40 cm thick iron shield, this ratio drops to 25% for point-kernel and 10% for MC solution.

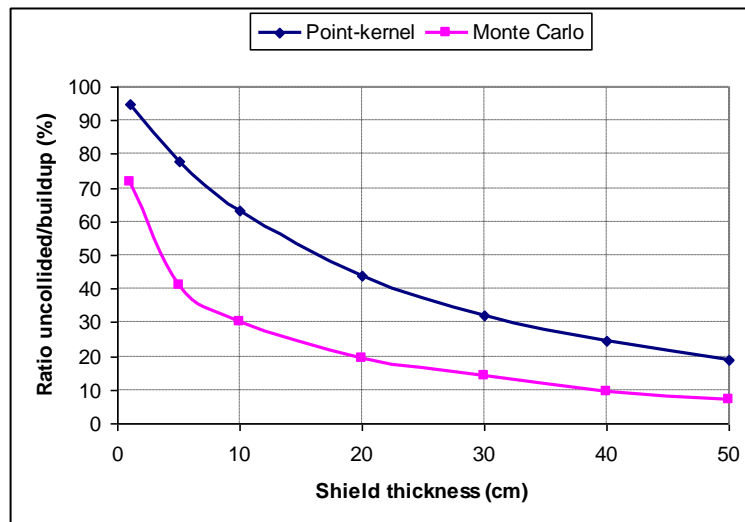


Figure 13: Ratio of uncollided to total gamma flux (10 MeV photons)

The flux relative error of point-kernel to MC solution in Figure 14 is also different for high energy photons. The uncollided flux ratio between point-kernel and MC is positive and below 20% even for 50 cm thick iron shield while the buildup flux ratio drops to a practically constant value of -50% for shield thicknesses above 10 cm. This is a clear indication how an uncollided flux is a more conservative from a point-kernel solution, while the higher MC buildup flux takes into an account a complete photon physical interaction.

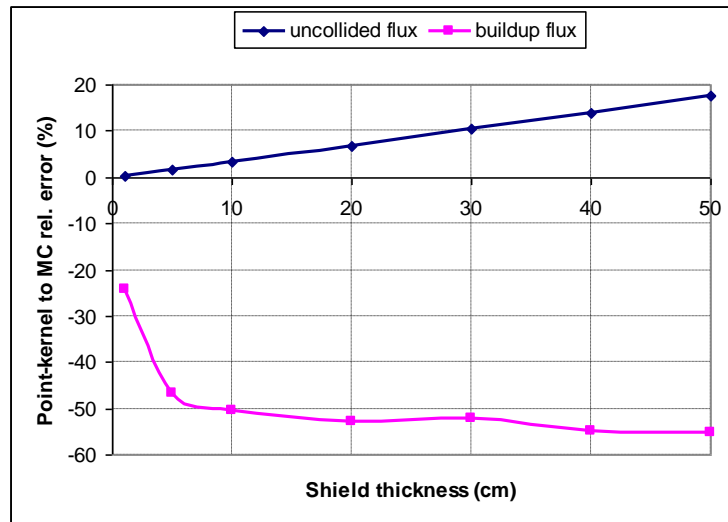


Figure 14: Relative error of point-kernel to MC solution (10 MeV photons)

The buildup factors in Figure 15 show again a high level of similarity but with much smaller values (range 1 to 6), since the high-energy photon scattering inside the shield is now less pronounced.

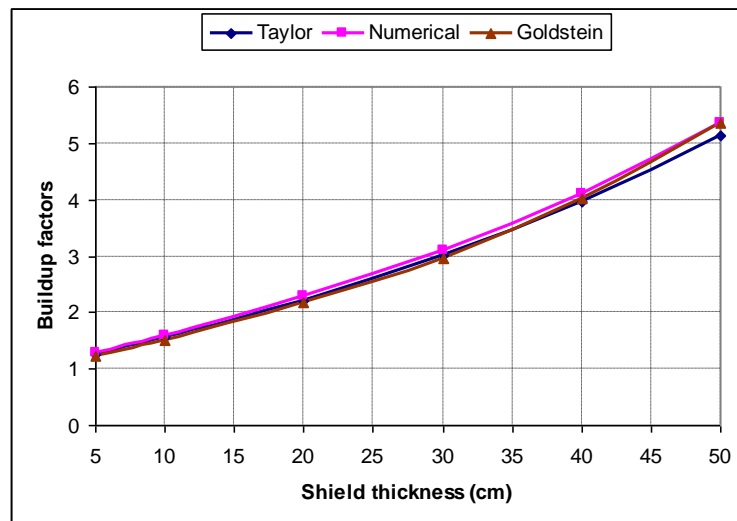


Figure 15: The buildup factors for 10 MeV photons inside iron shield

Finally, the mesh tally solution of gamma buildup flux with relative errors is shown in Figure 16 in $y=0$ plane, for the case of 50 cm iron shield and 10 MeV photons. The CADIS method was again used with 12.9 min of CPU time for VR preparation, Monaco MC took 8.4 min so total CPU time amounts to 21.3 min. The point-detector MC buildup flux was $6.04e-02$ phot/cm²/s with relative error 0.64%. For comparison, point-kernel solution gives smaller value of $2.70e-02$ phot/cm²/s with CPU time of 23 ms (speedup of cca 56000), since only a one-pass through program is needed to obtain an analytical solution.

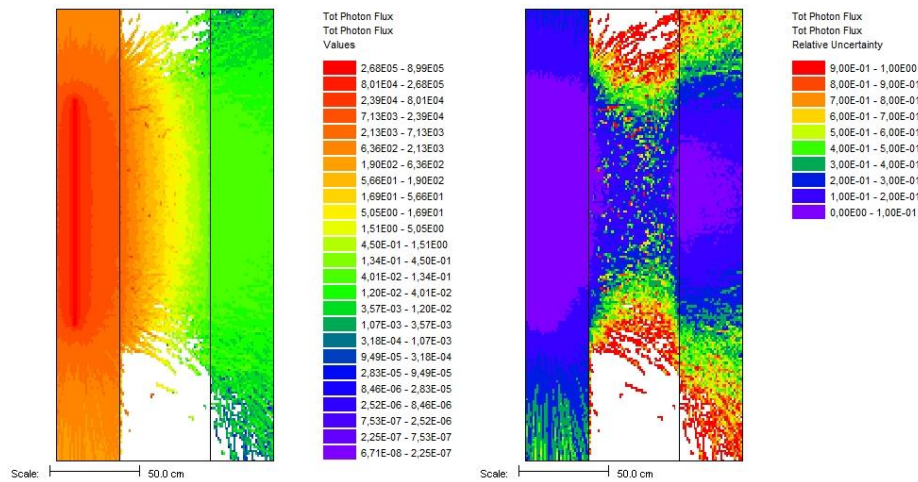


Figure 16: CADIS solution for 10 MeV photons and 50 cm thick iron shield

6 CONCLUSION

The application of the point-kernel method on an isotropic gamma line source, a slab iron shield and isotropic point detector was demonstrated through theoretical and numerical approach. The developed point-kernel code can be run in command prompt by manually entering data or by GUI interface program which assists users with input data preparation. The benchmark test cases were compared to a reference MC solution, with varying iron shield thickness in cm (1, 5, 10, 20, 30, 40, and 50) and enveloping gamma ray energies with 0.5 MeV and 10 MeV, for which available buildup factors were used. A close agreement of obtained results was noticed for small to medium shield thicknesses and obtained numerical buildup factors showed excellent agreement with theoretical Goldstein and Taylor datasets. However, typical point-kernel "conservatism" was noticed only for uncollided gamma flux component, while the total MC flux proved to be relatively higher for most of test cases. These findings clearly demonstrate limitations of neglecting various photon transport processes inside the shield, which are more than compensated with only a fraction of CPU time needed for point-kernel flux solution with an acceptable deviation. Future work will expand program and GUI capabilities to other source geometrical forms and composite (multilayered) shields which require specific steps in obtaining the so-called effective buildup factors of several different shielding materials.

REFERENCES

- [1] H. Khan, Use of Different Monte Carlo Sampling Techniques, RAND Corporation, P-766, 1955. As of May 23, 2024: <https://www.rand.org/pubs/papers/P766.html>
- [2] B. G. Carlson, K. D. Lathrop, Transport theory – The Method of Discrete Ordinates, in: H. Greenspan, C. N. Kelber, D. Okrent (eds), Computing Methods in Reactor Physics, Gordon & Breach, New York, 1968.
- [3] N. M. Schaeffer, Reactor Shielding for Nuclear Engineers, U.S. Atomic Energy Commission, Office of Information Services, 1973.
- [4] T. Rockwell III (Ed.), Reactor Shielding Design Manual, USAEC Report TID-7004, 1956.
- [5] H. Goldstein, Fundamental Aspects of Reactor Shielding, Reading, Mass., Addison-Wesley Pub. Co. 1959.

- [6] S. Glasstone, A. Sesonske, Nuclear Reactor Engineering - Reactor Design Basics, Fourth Edition Volume One, Chapman & Hall, New York, 1994.
- [7] M. Matijević, R. Ječmenica, D. Grgić, Spent Fuel Pool Dose Rate Calculations Using Point Kernel and Hybrid Deterministic-Stochastic Shielding Methods, *Journal of Energy*, 65 (2016), 1; 151-161.
- [8] K. Trontl, D. Pevec, M. Matijević, Monte Carlo Codes for Neutron Buildup Factors, *Journal of Energy*, 62 (2013), 1-4; 171-179.
- [9] P. Dučkić, K. Trontl, D. Grgić, M. Matijević, Point Kernel Modification Including Support Vector Regression Neutron Buildup Factor Models, *Journal of Energy*, 68 (2019), 2-3; 156-170.
- [10] B. W. Kernighan, D. M. Ritchie, The C Programming Language, 2nd Edition, Prentice Hall, 1988.
- [11] B. Stroustrup, The C++ Programming Language, Addison-Wesley Pub. Co. 2013.
- [12] Qt documentation available at: <https://doc.qt.io/>
- [13] "SCALE: A Comprehensive Modeling and Simulation Suite for Nuclear Safety Analysis and Design", ORNL/TM-2005/39, Version 6.1, June 2011. Available from Radiation Safety Information Computational Center at Oak Ridge National Laboratory as CCC-785.